OPEN

Experimental & Molecular Medicine (2014) 46, e77; doi:10.1038/emm.2013.151

www.nature.com/emm

ORIGINAL ARTICLE

# Knockdown of 14-3-3ζ enhances radiosensitivity and radio-induced apoptosis in CD133$^+$ liver cancer stem cells

Young Ki Lee, Wonhee Hur, Sung Won Lee, Sung Woo Hong, Sung Woo Kim, Jung Eun Choi and Seung Kew Yoon

**14-3-3ζ is related to many cancer survival cellular processes. In a previous study, we showed that silencing 14-3-3ζ decreases the resistance of hepatocellular carcinoma (HCC) to chemotherapy. In this study, we investigated whether silencing 14-3-3ζ affects the radioresistance of cancer stem-like cells (CSCs) in HCC. Knockdown of 14-3-3ζ decreased cell viability and the number of spheres by reducing radioresistance in CSCs after γ-irradiation (IR). Furthermore, the levels of pro-apoptotic proteins were upregulated in CSCs via silencing 14-3-3ζ after IR. These results suggest that 14-3-3ζ knockdown enhances radio-induced apoptosis by reducing radioresistance in liver CSCs.**
*Experimental & Molecular Medicine* (2014) **46,** e77; doi:10.1038/emm.2013.151; published online 21 February 2014

**Keywords:** 14-3-3ζ; apoptosis; cancer stem-like cell; hepatocellular carcinoma; radioresistance

## INTRODUCTION

Hepatocellular carcinoma (HCC) is a malignancy with a particularly poor prognosis because of its unresponsiveness to treatment.[1] Patients diagnosed with HCC at an early stage could be candidates for curative treatments with relatively high 5-year survival rates, such as surgical resection, radio-frequency ablation or liver transplantation,[2] but unfortunately, only 30–40% of newly diagnosed HCCs are suitable for curative treatment.[3] The majority of patients with HCC receive palliative treatments, such as transarterial chemoembolization, radiotherapy or sorafenib.[4–6] A combination of palliative treatment modalities is also favored in selected cases to increase the treatment response rates and ultimately the survival rate. In particular, radiotherapy has played an increasingly favorable role in the treatment of HCC with the development of radiation delivery techniques, such as three-dimensional conformal radiotherapy, stereotactic body radiotherapy and image-guided radiotherapy,[7] however, various adverse effects have also been reported. The failure of radiotherapy to cure HCC is caused not only by the radioresistance of tumor cells but also by its side effects. Moreover, a study by Cheng *et al.* demonstrated that radiation enhances the invasiveness of HCC by upregulating matrix metalloproteinase-9 protein levels through the phosphatidylinositol-3′-kinase/Akt and nuclear factor-κB signal transduction pathways.[8] Previous studies have described that radiation increases toxic substances, such as interleukin-6 and reactive oxygen species, in normal hepatocytes[9–11] by activating signaling pathways including epidermal growth factor receptor, phosphatidylinositol-3′-kinase, mitogen-activated protein kinase (MAPK), c-Jun-NH(2)-terminal kinase and p38 pathways as well as FAS-R and tumor necrosis factor receptor signaling to pro-caspases and nuclear factor-κB.[12] Therefore, radioresistance mechanisms have been actively investigated to improve the survival of patients with cancer, but the mechanisms underlying the development of radioresistance in HCC remain unclear.

Recent evidence suggests a correlation between the cancer stem-like cell (CSC) population with a high capacity for radioresistance and the non-CSC population.[13] In this regard, one of the factors for successful radiotherapy is the radiosensitivity of CSCs. A certain type of HCC cell expressing CD133, a pentaspan transmembrane cell-surface glycoprotein that marks a subset of CSCs in several tumor types, is also associated with radioresistance.[14,15] A study by Bao *et al.* demonstrated that checkpoint kinases, such as

Liver Research Center and WHO Collaborating Center of Viral hepatitis, Catholic University of Korea, Seoul, Korea
Correspondence: Professor SK Yoon, Department of Internal Medicine, Seoul St. Mary's Hospital, Catholic University of Korea, #505 Banpo-Dong, Seoul 137-040, Korea.
E-mail: yoonsk@catholic.ac.kr
Received 9 June 2013; revised 30 August 2013; accepted 15 October 2013

Chk1 and Chk2, are more predominantly activated in repair mechanisms in CD133+ glioma cells compared with CD133− cells.[16] We have previously reported that such radioresistance is also associated with activation of the MAPK/extracellular regulated kinase (ERK) survival pathway.[17] Furthermore, a recent report suggested that the Wnt/β-catenin pathway may contribute to radioresistance in breast cancer.[18] The role of CSCs in hepatocarcinogenesis has been reported in several studies.[15,19] CSCs are cancer cells with the stemness characteristics of stem cells such as self-renewal and differentiation. CSCs have been hypothesized to influence the prognosis of patients by contributing to the development of recurrence, metastasis and drug resistance.[20–22] Therefore, developing strategies that target CSCs may lead to a better treatment response in patients with HCC.

The 14-3-3 proteins are a class of regulatory proteins that are involved in regulating apoptosis, cell cycle progression and mitogenic signaling.[23] Although the direct role of 14-3-3ζ has not been precisely clarified, Niemantsverdriet *et al.* reported that 14-3-3ζ has oncogenic properties, that downregulation of 14-3-3ζ sensitizes cells to stress-induced apoptosis and that ultraviolet-γ radiation increases the apoptosis rate by eightfold in 14-3-3ζ downregulated cells.[24]

We have previously reported that the 14-3-3ζ protein is significantly overexpressed in HCC cells and tissues and that suppressing 14-3-3ζ results in increased chemosensitivity to *cis*-diamminedichloridoplatinum (CDDP) in hepatoma cell lines.[25] However, whether silencing 14-3-3ζ affects radioresistance in relation to CSCs in HCC remains unclear. Accordingly, we investigated the effects of 14-3-3ζ knockdown on the molecular mechanism of radioresistance in CD133+ liver CSCs in the present study.

## MATERIALS AND METHODS

### Cell culture and γ-irradiation (IR)

Human hepatoma cells (Huh7) were grown in Dulbecco's modified Eagle's medium (DMEM; Invitrogen, Carlsbad, CA, USA) supplemented with 10% fetal bovine serum (Invitrogen), 100 μg ml$^{-1}$ penicillin and 0.25 μg ml$^{-1}$ streptomycin (Invitrogen) and were maintained in a humidified incubator at 37 °C with 5% $CO_2$. Cells were pre-incubated with serum-free DMEM and irradiated at 15 Gy using a cesium-137 source delivering 3.1 Gy min$^{-1}$ (Gammacell 3000 Elan irradiator; Best Theratronics, Ottawa, ON, Canada) in a conical tube before plating the cells in dishes or flasks. Then the cells were counted and plated using the same density.

### Flow cytometry

Cells were harvested with 0.5 mM trypsin/EDTA (Invitrogen), incubated at 4 °C with phycoerythrin-conjugated anti-CD133/1 antibody (Miltenyi Biotec, Auburn, CA, USA), and analyzed with a FACSCalibur cell sorter (BD Biosciences, Pharmingen, San Jose, CA, USA). The CD133+ and CD133− cells were sorted using the FACSCalibur cell sorter. Isotype-matched mouse IgG was used as a control.

### Sphere formation assay

Cells were plated in multiple ultralow attachment 24-well plates (Costar, Corning, NY, USA) at a density of 100 cells per well in serum-free DMEM/F12 (Invitrogen) with B27 supplement (Invitrogen), basic fibroblast growth factor (20 ng ml$^{-1}$; PeproTech, Rocky Hill, NJ, USA) and epidermal growth factor (20 ng ml$^{-1}$; PeproTech). The cells were incubated in a humidified incubator at 37 °C with 5% $CO_2$ and monitored for 5 days. The number of spheres (diameter > 50 μm) per well in four wells was counted using an inverted microscope (Olympus, Tokyo, Japan). The average sphere numbers was attained from these three independent experiments.

### Generation of stable short-hairpin small interfering RNA (shRNA) 14-3-3ζ infectants

In a previous study, we generated three stable 14-3-3ζ knockdown cell lines using a shRNA lentiviral vector (LV; Sigma-Aldrich, St Louis, MO, USA) and puromycin (Sigma-Aldrich) selection.[25] Three shRNA LVs were designed to target positions 232, 349 and 637 in the human *14-3-3ζ* gene (GenBank Accession No. NM_176875.2), and one of these vectors was selected. The shRNA negative control-lentiviral particle (LV-NC) was used as the negative control (NC). To generate stable cells, Huh7 cells were plated in 12-well plates ($1 \times 10^5$ cells per well), transduced with 5 multiplicity of infection (MOI) lentiviral particles using 8 μg ml$^{-1}$ hexadimethrine bromide (Sigma-Aldrich) and incubated in DMEM containing puromycin (10 μg ml$^{-1}$) for screening at 37 °C with 5% $CO_2$. Suppression of 14-3-3ζ in stable cells was confirmed by western blot analysis.

### Western blot analysis

Protein extracts were separated by 10 and 12% SDS-polyacrylamide gel electrophoresis, transferred to nitrocellulose membranes (Schleicher & Schuell, Dassel, Germany) and blocked in 5% skim milk. Primary antibodies were used as indicated by the manufacturer and are as follows: monoclonal anti-β-actin (Sigma-Aldrich), polyclonal anti-14-3-3ζ (Santa Cruz Biotechnology, Santa Cruz, CA, USA), polyclonal anti-CD133 (Santa Cruz Biotechnology), polyclonal anti-Bax (DAKO, Carpinteria, CA, USA), polyclonal anti-cleaved caspase-3 (Cell Signaling Technologies, Danvers, MA, USA) and monoclonal anti-poly ADP-ribose polymerase (BD Biosciences Pharmingen). The blots were treated overnight at 4 °C with the primary antibodies. The membranes were washed with Tris-buffered saline (TBS) containing 0.05% Tween-20 and incubated with horseradish peroxidase-conjugated anti-mouse, anti-rabbit or anti-goat secondary antibodies (Amersham Biosciences, Cardiff, UK). Protein bands were visualized using an enhanced chemiluminescence system (Amersham Pharmacia Biotech, Uppsala, Sweden) according to the manufacturer's instructions.

### Cell viability assays

Cell viability was evaluated with the Cell Titer 96 AQueous Assay (Promega, Madison, WI, USA). The Cell Titer 96 AQueous Assay is composed of solutions of a novel tetrazolium compound (3-(4,5-dimethylthiazol-2-yl)-5-(3-carboxymethoxyphenyl)-2-(4-sulfophenyl)-2H-tetrazolium, inner salt; MTS) and an electron coupling reagent (phenazine methosulfate). Cells were plated in multiple 96-well plates at a density of 5000 cells per well. Absorbance was measured at 490 nm using a SpectraMax 250 microplate reader (Molecular Devices, Sunnyvale, CA, USA).

### Apoptosis assays and luminometric caspase-3/7 activity test

Apoptosis was detected by Annexin V/propidium iodide (PI) staining (BD BioSciences) according to the manufacturer's instructions. In total, 10 000 cells were counted by flow cytometry using a fluorescence-activated cell sorter (Becton-Dickinson, San Jose, CA, USA).

The resulting data were analyzed using Summit 5.2 software (Beckman Coulter Inc., Miami, FL, USA). Caspase-3/7 activity was measured in cells using Caspase-Glo 3/7 (Promega) following the manufacturer's protocol. Luminescence was measured using a SpectraMax 250 microplate reader.

### Immunofluorescence staining

Cells were fixed in methanol/formaldehyde solution for 15 min in the cleaved caspase-3 immunofluorescence assay. The fixed cells were incubated with anti-cleaved caspase-3 (1:200; Cell Signaling Technologies), followed by incubation with Alexa 488-labeled anti-rabbit IgG (1:1000; LifeTechnologies, Carlsbad, CA, USA). The cells were stained with 4′-6-diamidino-2-phenylindole (Sigma-Aldrich) to counterstain the nuclei and were then examined by fluorescence microscopy (Olympus).

### Statistical analysis

All experiments were performed at least three times. Statistical comparisons were performed by analysis of variance using SPSS 13.0 software (SPSS, Chicago, IL, USA). A *P*-value $<0.05$ was considered significant.

## RESULTS

### 14-3-3ζ expression is upregulated in liver CSCs after IR

We previously demonstrated that 14-3-3ζ has an important role in the development of HCC and that silencing the 14-3-3ζ gene enhances the chemosensitivity effect of CDDP in HCC.[25] In the present study, we investigated whether the knockdown of 14-3-3ζ expression is also associated with radioresistance in liver CSCs.

First, we conducted a sphere-forming assay to confirm whether CD133$^+$ hepatoma cells have the stemness characteristic of CSCs (Figure 1a). More spheres were counted in CD133$^+$ liver CSCs than in CD133$^-$ cells ($P<0.05$; Figure 1a). In contrast, a slight decrease in both CD133$^+$ and CD133$^-$ cells was observed after IR. Notably, the size of spheres decreased in IR-exposed cells compared with non-exposed cells. These results indicate that only CD133$^+$ hepatoma cells have self-renewal and differentiation capacity. Therefore, we used CD133$^+$ hepatoma cells for further analyses.

A western blot analysis was performed after IR to confirm whether 14-3-3ζ expression was regulated between CD133$^+$

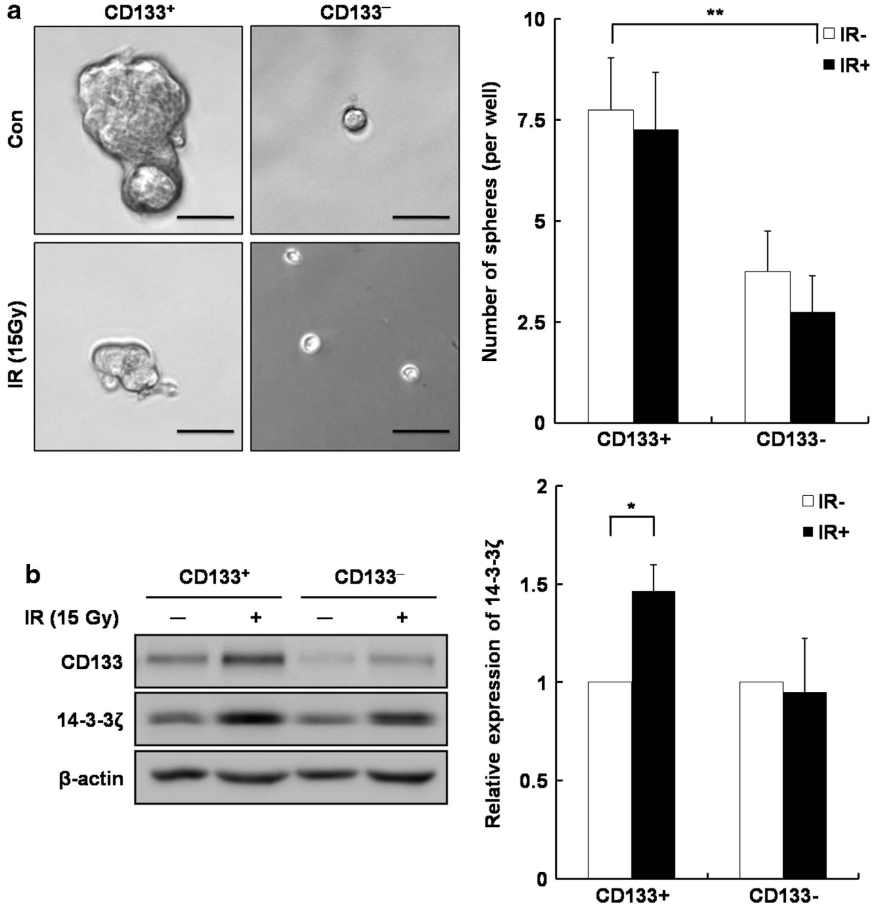


**Figure 1** Correlation of stemness characteristics with 14-3-3ζ expression in CD133$^+$ and CD133$^-$ hepatoma cells after γ-irradiation (IR). (**a**) Representative phase-contrast micrographs of tumor spheres formed in CD133$^+$ and CD133$^-$ cells at 96 h after IR. Black bars, 50 μm. Sphere formation efficiency is represented by a quantitative analysis. The number of spheres (diameter $>50$ μm) from 100 cells was counted at 96 h after IR. The data are the mean ± s.d of three independent experiments (**$P<0.01$). (**b**) 14-3-3ζ expression was analyzed by western blot using a 14-3-3ζ antibody in CD133$^+$ and CD133$^-$ cells at 96 h after IR. Band densities were quantified with TINA imaging analysis software and normalized to β-actin expression. The data represent the relative density of IR and were reproduced in three independent experiments (*$P<0.05$). Con, control.

and CD133$^-$ cells after IR (Figure 1b). 14-3-3ζ expression was upregulated by approximately 1.5-fold in CD133$^+$ cells after IR compared with non-exposed CD133$^+$ cells ($P<0.05$; Figure 1b). However, no significant difference in 14-3-3ζ expression was noted between CD133$^-$ and IR-exposed CD133$^-$ cells. In addition, 14-3-3ζ expression was similar between CD133$^+$ and CD133$^-$ cells. These results indicate that 14-3-3ζ acts on liver CSCs when hepatoma cells are treated with IR.

**Silencing 14-3-3ζ in liver CSCs using LVs**

We established cell lines using LVs containing shRNAs of NC and 14-3-3ζ (Zeta) to silence 14-3-3ζ. After silencing 14-3-3ζ, expression in LV-NC and LV-Zeta cells was analyzed by western blot analysis (Figure 2a). 14-3-3ζ expression decreased by approximately 70% in LV-Zeta cells compared with LV-NC cells ($P<0.01$; Figure 2a). We also determined whether 14-3-3ζ silencing was retained after cell sorting with an anti-CD133/1 antibody. The LV-NC and LV-Zeta cells were sorted into CD133$^+$ (LV-NC$^{CD133+}$ and LV-Zeta$^{CD133+}$) and CD133$^-$ (LV-NC$^{CD133-}$ and LV-Zeta$^{CD133-}$) cells, and protein expression in LV-NC and LV-Zeta cells was analyzed by western blot analysis. 14-3-3ζ expression in both LV-Zeta$^{CD133+}$ and LV-Zeta$^{CD133-}$ cells decreased compared with LV-NC$^{CD133+}$ and LV-NC$^{CD133-}$ cells (Figure 2b). These results show that the silencing of 14-3-3ζ was maintained in hepatoma cells after sorting.

**Silencing 14-3-3ζ inhibits cell viability and stemness after IR by reducing radioresistance in liver CSCs**

We explored whether silencing 14-3-3ζ would affect the stemness characteristics of CSCs and cell viability in CD133$^+$ liver CSCs after IR exposure. We performed the MTS assay in IR-exposed LV-NC and LV-Zeta cells after sorting to evaluate cell viability. The viability of CD133$^-$ cells significantly decreased after IR compared with CD133$^+$ cells because of radiosensitivity (data not shown). Cell viability decreased compared with non-exposed cells at 96 h after IR ($P<0.05$; Figure 3a). Notably, the cell viability of LV-Zeta$^{CD133+}$ cells decreased significantly compared with LV-NC$^{CD133+}$ cells at 96 h after IR ($P<0.05$; Figures 3a and b). However, no significant difference was observed between LV-NC$^{CD133-}$ and LV-Zeta$^{CD133-}$ cells at 96 h after IR (data not shown). These results suggest that silencing 14-3-3ζ inhibited cell viability in CD133$^+$ liver CSCs after IR by reducing radioresistance.

A sphere-forming assay was conducted to identify whether the silencing of 14-3-3ζ would affect the self-renewal and differentiation capacity of CD133$^+$ liver CSCs. Significantly fewer LV-Zeta$^{CD133+}$ spheres were detected compared with LV-NC$^{CD133+}$ cells ($P<0.01$; Figure 3c). However, no significant difference in the number of spheres was observed between LV-NC $^{CD133+}$ and IR-exposed LV-NC$^{CD133+}$ cells. Moreover, the number of spheres decreased significantly in IR-exposed LV-Zeta$^{CD133+}$ cells compared with unexposed LV-Zeta$^{CD133+}$ cells ($P<0.05$; Figure 3c). These results suggest that silencing 14-3-3ζ reduces the stemness characteristics of liver CSCs after radiation, resulting in diminished radioresistance in HCC.

**Knockdown of 14-3-3ζ enhances radiation-induced apoptosis in liver CSCs**

The MTS assay revealed that CD133$^+$ liver CSCs maintained their cell viability after IR compared with CD133$^-$ cells. However, IR-exposed LV-Zeta$^{CD133+}$ cells showed a reduced cell viability via diminished radioresistance. Annexin V-PI staining was performed to determine whether cell viability and/or cell death were affected by silencing 14-3-3ζ after IR.

The number of apoptotic cells (Annexin V-positive cells) increased in both LV-NC and LV-Zeta cells after IR, but no significant difference in the necrotic cells (PI-positive and Annexin V-negative cells) was noted between the groups (Figure 4a). The number of early apoptotic cells (Annexin V-positive and PI-negative cells) was approximately 3.5-fold greater in the LV-Zeta$^{CD133+}$ group than the LV-NC$^{CD133+}$ group ($P<0.05$; Figure 4a). However, no significant difference

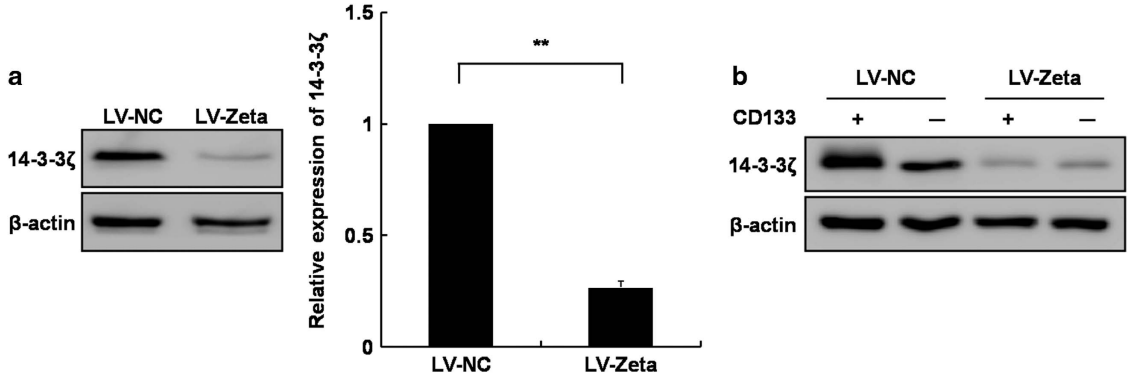


**Figure 2** Knockdown of 14-3-3ζ expression in the negative control-lentiviral particle (LV-NC) and LV-Zeta cells. (**a**) Protein lysates from LV-NC and LV-Zeta cells were analyzed by western blot analysis using a 14-3-3ζ antibody. The band densities were quantified with TINA imaging analysis software and normalized to β-actin expression. The data are expressed relative to the density of NC and were reproduced in three independent experiments (**$P<0.01$). (**b**) LV-NC and LV-Zeta cells were sorted into CD133$^+$ and CD133$^-$ cells. 14-3-3ζ expression was analyzed by western blot analysis in sorted LV-NC and LV-Zeta cells.

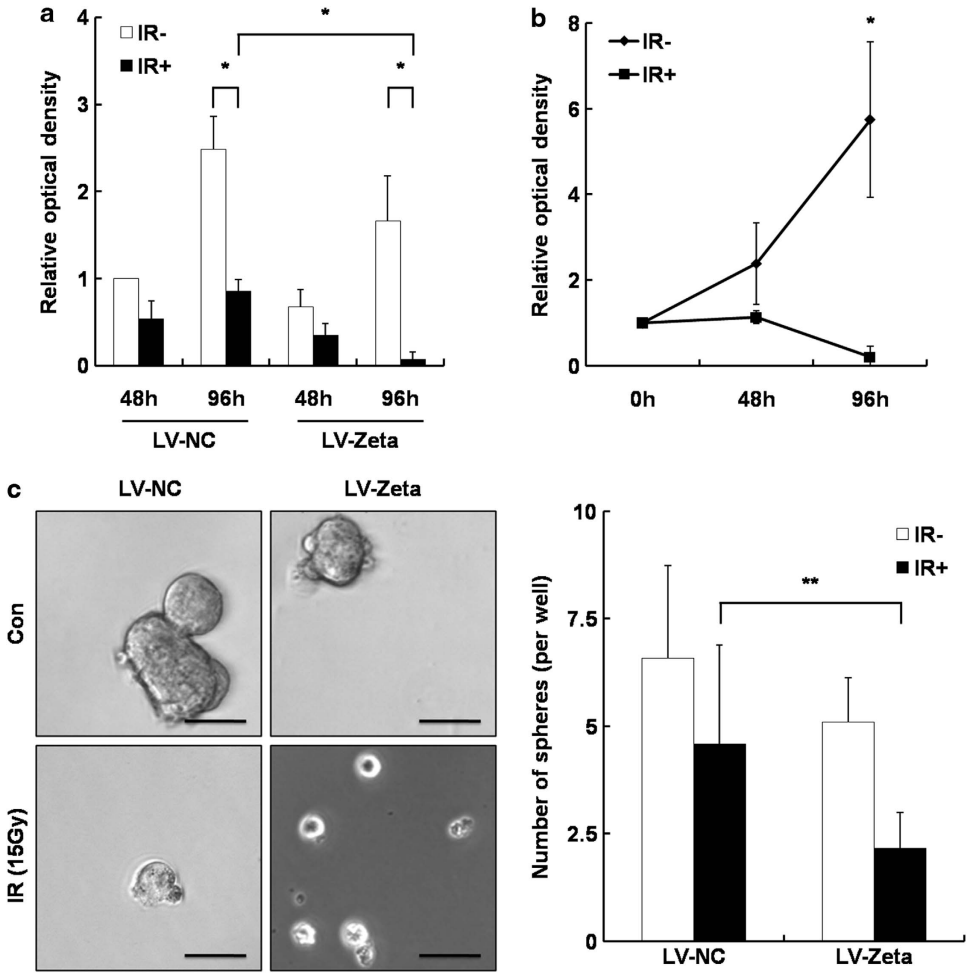


**Figure 3** The capacity of cell viability and stemness in γ-irradiation (IR)-exposed negative control-lentiviral particle (LV-NC) and LV-Zeta cells. The MTS assay was performed at 0, 48 and 96 h in IR-exposed cells to investigate cell viability in LV-NC and LV-Zeta cells. (**a**) CD133+ cell viability was measured at 48 and 96 h after IR. The capacity to proliferate was represented relative to the absorbance of LV-NC cells at 48 h after IR. (**b**) The graph shows the cell viability of LV-Zeta$^{CD133+}$ cells at 96 h after IR. The rate of cell viability is presented relative to the absorbance of unexposed cells at 0 h. The results represent the mean ± s.d. of three independent experiments (*$P<0.05$). (**c**) A sphere formation assay was performed after IR to verify the stemness characteristic in IR-exposed LV-NC and LV-Zeta cells. Representative phase-contrast micrographs of tumor spheres formed in LV-NC$^{CD133+}$ and LV-Zeta$^{CD133+}$ cells at 96 h after IR. Black bar, 50 μm. Sphere formation efficiency is represented by a quantitative analysis. The number of spheres (diameter > 50 μm) from 100 cells was counted at 96 h after IR. The results are the mean ± s.d. of three independent experiments (**$P<0.01$). Con, control.

was observed in the early apoptotic cells between LV-NC$^{CD133-}$ and LV-Zeta$^{CD133-}$ cells (Supplementary Figure 1A). These results indicate that silencing 14-3-3ζ enhanced the radiation-induced apoptosis in CD133+ liver CSCs. Next, a western blot analysis was performed to further confirm the involvement of pro-apoptotic proteins, such as Bax, caspase-3 and poly ADP-ribose polymerase, in radio-induced apoptosis by 14-3-3ζ knockdown. Cleaved caspase-3 and Bax expression increased more in LV-Zeta$^{CD133+}$ cells compared with LV-NC$^{CD133+}$ cells after IR ($P<0.05$; Figure 4b). However, poly ADP-ribose polymerase expression increased only slightly in LV-Zeta$^{CD133+}$ cells compared with LV-NC$^{CD133+}$ cells after IR, but no significant difference was observed. No significant differences were noted between the control and IR-exposed CD133− cells. These results indicate that silencing 14-3-3ζ enhanced radiation-induced apoptosis in liver CSCs after IR.

We measured caspase-3/7 activity to determine whether radio-induced apoptosis was increased by 14-3-3ζ knockdown. Caspase-3/7 activity was significantly greater in LV-Zeta$^{CD133+}$ cells than in LV-NC $^{CD133+}$ cells after IR ($P<0.05$; Figure 5a). However, no differences in caspase-3/7 activity were observed between LV-NC$^{CD133-}$ and LV-Zeta$^{CD133-}$ cells after IR (Supplementary Figure 1B). In addition, we performed immunofluorescence staining of cleaved caspase-3 to verify apoptosis. The nuclei were more condensed, and cleaved caspase-3-positive cells were detected more predominantly in IR-exposed cells than in non-IR exposed cells. Cleaved caspase-3

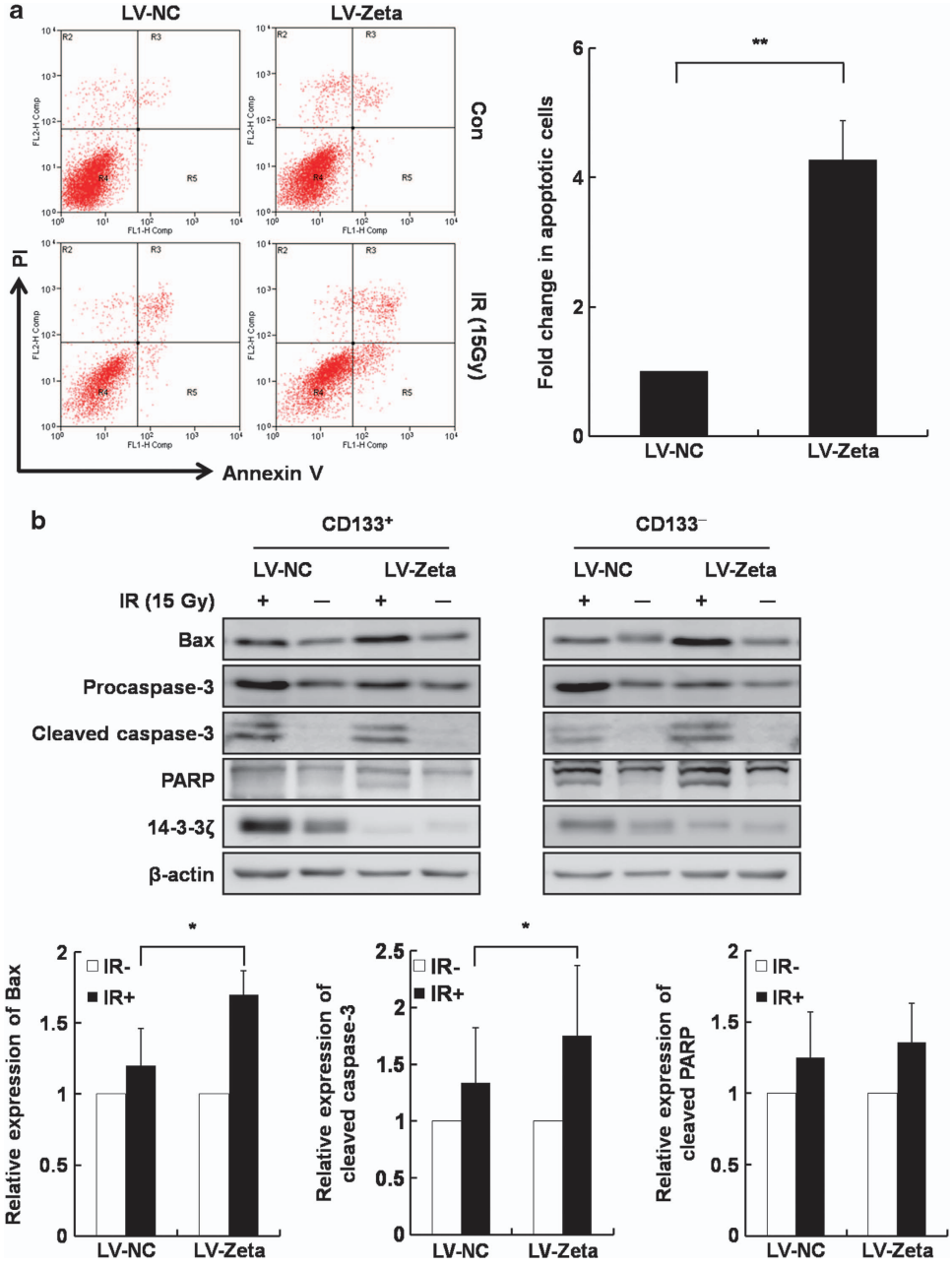


**Figure 4** Radio-induced apoptosis and expression of pro-apoptotic proteins in negative control-lentiviral particle (LV-NC) and LV-Zeta cells after γ-irradiation (IR). (**a**) Apoptotic cell death was measured by flow-assisted cytometry analysis with fluorescein isothiocyanate-conjugated Annexin V/propidium iodide staining at 96 h after IR to determine radio-induced apoptosis in LV-NC$^{CD133+}$ and LV-Zeta$^{CD133+}$ cells. The lower right quadrant indicates early apoptotic cells, and the upper right quadrant indicates late apoptotic cells. The early apoptotic cells are represented by a quantitative analysis. The results are the mean ± s.d. of three independent experiments (**$P<0.01$). (**b**) Protein lysates were analyzed by western blot analysis using Bax, cleaved caspase-3 and poly ADP-ribose polymerase (PARP) antibodies in LV-NC$^{CD133+}$ and LV-Zeta$^{CD133+}$ cells at 96 h after IR. The band densities were quantified with TINA imaging analysis software and normalized to β-actin expression. The data are expressed relative to the density of IR- and were reproduced in three independent experiments (*$P<0.05$).

was detected at greater levels in the LV-Zeta$^{CD133+}$ cells compared with LV-NC$^{CD133+}$ cells after IR (Figure 5b), but no significant difference was observed between LV-Zeta$^{CD133-}$ and LV-NC$^{CD133-}$ cells (data not shown). These results suggest that 14-3-3ζ knockdown increased caspase-3/7 activity and enhanced radiation-induced apoptosis in liver CSCs.

## DISCUSSION

HCC is a highly malignant tumor with a poor prognosis despite several therapeutic strategies including radiation therapy.[26] The role of radiation therapy in cancer treatment is to suppress tumor growth by inhibiting cell viability and inducing apoptosis.[27] Thus, radiation therapy has been widely

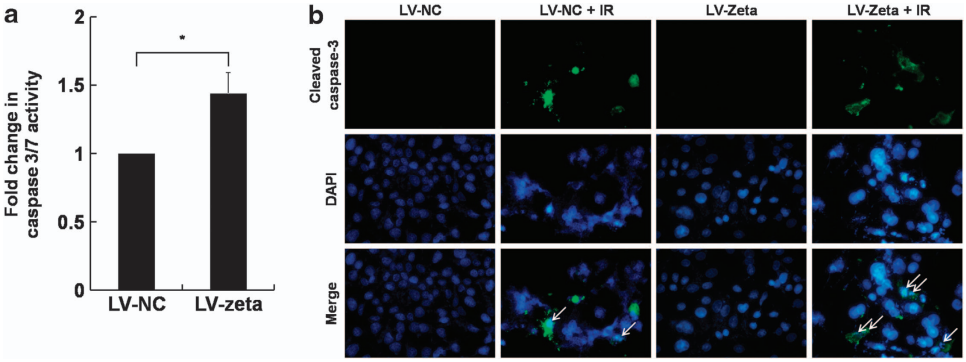


**Figure 5** Caspase-3/7 activity and cleaved caspase-3 expression in negative control-lentiviral particle (LV-NC) and LV-Zeta cells after γ-irradiation (IR). (**a**) Caspase-3/7 activities were measured by luminescence in LV-NC$^{CD133+}$ and LV-Zeta$^{CD133+}$ cells at 96 h after IR. The data are expressed relative to the luminescence of LV-NC cells and were reproduced in three independent experiments (*$P<0.05$). (**b**) Cleaved caspase-3 (green) expression was measured by immunofluorescence staining in LV-NC$^{CD133+}$ and LV-Zeta$^{CD133+}$ cells at 96 h after IR. The nuclei were stained with 4′-6-diamidino-2-phenylindole (DAPI; blue). Original magnification, ×200.

applied to various types of cancer, but its therapeutic efficiency remains limited because of radiotoxicity in non-tumorous tissue and radioresistance in tumorous tissue. Recent studies have reported that restricted subsets of tumor cells, defined as CSCs, share characteristics with normal stem cells but are related to chemo- and radioresistance.[28–30] However, whether this radioresistant subpopulation possesses stemness characteristics in HCC is not completely understood.

In our previous study, we reported that CD133$^+$ cells showing CSC stemness characteristics are associated with radioresistance in HCC.[17] These results suggest that increased CD133$^+$ cell proliferation following IR may be due to activation of the survival-promoting ERK/MAPK pathway.

The MAPK/ERK signaling pathway is involved in cell progression and is activated by various proteins, such as 14-3-3ζ proteins.[31] In particular,14-3-3ζ expression is upregulated in various types of malignancies, including oral cancer,[32] breast cancer,[33] lung carcinoma and HCC.[34,35] In addition, the silencing of 14-3-3ζ increases the radiosensitivity of ultraviolet irradiation and increases apoptosis eightfold in lung cancer.[24] In our previous study, we also demonstrated that silencing 14-3-3ζ inhibits tumor growth and enhances chemosensitivity to CDDP.[25] These results suggest that 14-3-3ζ influences chemosensitivity to CDDP by regulating the c-Jun-NH(2)-terminal kinase and p38/MAPK pathways.

In this study, we determined whether 14-3-3ζ is associated with the mechanism of radioresistance in liver CSCs. As shown in Figure 1, 14-3-3ζ expression levels in CD133$^+$ cells were more upregulated than CD133$^-$ cells post IR. These results suggest that 14-3-3ζ in liver CSCs has a particular role in radioresistance in HCC.

CSCs possess several features associated with resistance to DNA damage, including increased DNA repair capacity and resistance to apoptosis.[36] We further investigated whether expression of 14-3-3ζ is involved in regulating stemness, cell viability and apoptosis resistance in CSCs by establishing a 14-3-3ζ stable knockdown Huh7 cell line using a lentiviral shRNA.[25]

We found that silencing 14-3-3ζ affected the cell viability of liver CSCs following exposure to IR. CSCs have extensive cell viability and a high survival rate because of their strong radioresistant characteristics after IR. We found that down-regulation of 14-3-3ζ in liver CSCs may increase the sensitivity to IR and significantly decrease cell viability following IR exposure (Figure 3). Furthermore, we observed an increased rate of apoptosis after IR in the CSCs following knockdown of 14-3-3ζ, resulting in reduced radioresistance. Moreover, 14-3-3ζ knockdown enhanced radiation-induced apoptosis and was accompanied by high amounts of cleaved caspase-3 and Bax in liver CSCs. This observation was also confirmed by previous studies showing that the silencing of 14-3-3ζ increases Bax activation.[37,38] In addition, previous studies have reported that 14-3-3ζ is involved in apoptosis via interactions with proteins related to the mitochondrial permeability transition and apoptosis.[39–41] Thus, our results suggest that suppressing 14-3-3ζ inhibited cell viability and enhanced radiation-induced apoptosis via interactions with Bax, leading to reduced radioresistance.

An exploration of the mechanism underlying cellular and molecular radioresistance is essential to improve the therapeutic efficacy of radiation therapy for HCC. In this regard, our findings show that the expression of 14-3-3ζ may be involved in the response to IR and that the knockdown of 14-3-3ζ reduced the radioresistant characteristics of CSCs. We also demonstrated that stable depletion of 14-3-3ζ reduced CSC stemness and enhanced radio-induced apoptosis following IR exposure. In conclusion, regulating 14-3-3ζ expression may contribute to the therapeutic efficacy of radiation therapy for HCC.

## ACKNOWLEDGEMENTS

This research was supported by a grant from the Basic Science Research Program through the National Research Foundation of Korea (NRF) funded by the Ministry of Education, Science and Technology (2011-0027071) and the Korean Health Technology R&D Project, Ministry of Health and Welfare, Korea (NO. 2011-08-0168-A0094).

1 Block TM, Mehta AS, Fimmel CJ, Jordan R. Molecular viral oncology of hepatocellular carcinoma. *Oncogene* 2003; **22:** 5093–5107.
2 Llovet JM, Bru C, Bruix J. Prognosis of hepatocellular carcinoma: the BCLC staging classification. *Semin Liver Dis* 1999; **19:** 329–338.
3 Sala M, Llovet JM, Vilana R, Bianchi L, Sole M, Ayuso C *et al.* Initial response to percutaneous ablation predicts survival in patients with hepatocellular carcinoma. *Hepatology*, Baltimore, MD 2004; **40:** 1352–1360.
4 Kane RC, Farrell AT, Madabushi R, Booth B, Chattopadhyay S, Sridhara R *et al.* Sorafenib for the treatment of unresectable hepatocellular carcinoma. *Oncologist* 2009; **14:** 95–100.
5 Camma C, Schepis F, Orlando A, Albanese M, Shahied L, Trevisani F *et al.* Transarterial chemoembolization for unresectable hepatocellular carcinoma: meta-analysis of randomized controlled trials. *Radiology* 2002; **224:** 47–54.
6 Llovet JM, Ricci S, Mazzaferro V, Hilgard P, Gane E, Blanc JF *et al.* Sorafenib in advanced hepatocellular carcinoma. *N Engl J Med* 2008; **359:** 378–390.
7 Ursino S, Greco C, Cartei F, Colosimo C, Stefanelli A, Cacopardo B *et al.* Radiotherapy and hepatocellular carcinoma: update and review of the literature. *Eur Rev Med Pharmacol Sci* 2012; **16:** 1599–1604.
8 Cheng JC, Chou CH, Kuo ML, Hsieh CY. Radiation-enhanced hepatocellular carcinoma cell invasion with MMP-9 expression through PI3K/Akt/NF-kappaB signal transduction pathway. *Oncogene* 2006; **25:** 7009–7018.
9 Maity A, Kao GD, Muschel RJ, McKenna WG. Potential molecular targets for manipulating the radiation response. *Int J Rad Oncol Biol Phys* 1997; **37:** 639–653.
10 Chou CH, Chen PJ, Lee PH, Cheng AL, Hsu HC, Cheng JC. Radiation-induced hepatitis B virus reactivation in liver mediated by the bystander effect from irradiated endothelial cells. *Clin Cancer Res* 2007; **13:** 851–857.
11 Chetty C, Bhoopathi P, Rao JS, Lakka SS. Inhibition of matrix metalloproteinase-2 enhances radiosensitivity by abrogating radiation-induced FoxM1-mediated G2/M arrest in A549 lung cancer cells. *Int J Cancer* 2009; **124:** 2468–2477.
12 Dent P, Yacoub A, Contessa J, Caron R, Amorino G, Valerie K *et al.* Stress and radiation-induced activation of multiple intracellular signaling pathways. *Radiat Res* 2003; **159:** 283–300.
13 Phillips TM, McBride WH, Pajonk F. The response of CD24(-/low)/CD44 + breast cancer-initiating cells to radiation. *J Natl Cancer Inst* 2006; **98:** 1777–1785.
14 Weigmann A, Corbeil D, Hellwig A, Huttner WB. Prominin, a novel microvilli-specific polytopic membrane protein of the apical surface of epithelial cells, is targeted to plasmalemmal protrusions of non-epithelial cells. *Proc Natl Acad Sci USA* 1997; **94:** 12425–12430.
15 Ma S, Chan KW, Hu L, Lee TK, Wo JY, Ng IO *et al.* Identification and characterization of tumorigenic liver cancer stem/progenitor cells. *Gastroenterology* 2007; **132:** 2542–2556.
16 Bao S, Wu Q, McLendon RE, Hao Y, Shi Q, Hjelmeland AB *et al.* Glioma stem cells promote radioresistance by preferential activation of the DNA damage response. *Nature* 2006; **444:** 756–760.
17 Piao LS, Hur W, Kim TK, Hong SW, Kim SW, Choi JE *et al.* CD133 + liver cancer stem cells modulate radioresistance in human hepatocellular carcinoma. *Cancer Lett* 2012; **315:** 129–137.
18 Woodward WA, Chen MS, Behbod F, Alfaro MP, Buchholz TA, Rosen JM. WNT/beta-catenin mediates radiation resistance of mouse mammary progenitor cells. *Proc Natl Acad Sci USA* 2007; **104:** 618–623.
19 Suetsugu A, Nagaki M, Aoki H, Motohashi T, Kunisada T, Moriwaki H. Characterization of CD133 + hepatocellular carcinoma cells as cancer stem/progenitor cells. *Biochem Biophys Res Commun* 2006; **351:** 820–824.
20 Reya T, Morrison SJ, Clarke MF, Weissman IL. Stem cells, cancer, and cancer stem cells. *Nature* 2001; **414:** 105–111.
21 Dean M, Fojo T, Bates S. Tumour stem cells and drug resistance. *Nat Rev Cancer* 2005; **5:** 275–284.
22 Sakariassen PO, Immervoll H, Chekenya M. Cancer stem cells as mediators of treatment resistance in brain tumors: status and controversies. *Neoplasia*, New York, NY 2007; **9:** 882–892.
23 Hermeking H. The 14-3-3 cancer connection. Nature reviews. *Cancer* 2003; **3:** 931–943.
24 Niemantsverdriet M, Wagner K, Visser M, Backendorf C. Cellular functions of 14-3-3 zeta in apoptosis and cell adhesion emphasize its oncogenic character. *Oncogene* 2008; **27:** 1315–1319.
25 Choi JE, Hur W, Jung CK, Piao LS, Lyoo K, Hong SW *et al.* Silencing of 14-3-3zeta over-expression in hepatocellular carcinoma inhibits tumor growth and enhances chemosensitivity to cis-diammined dichloridoplatium. *Cancer Lett* 2011; **303:** 99–107.
26 Aguayo A, Patt YZ. Nonsurgical treatment of hepatocellular carcinoma. *Semin Oncol* 2001; **28:** 503–513.
27 Fu KK, Phillips TL. Biologic rationale of combined radiotherapy and chemotherapy. *Hematol Oncol Clin North Am* 1991; **5:** 737–751.
28 Jordan CT, Guzman ML, Noble M. Cancer stem cells. *N Engl J Med* 2006; **355:** 1253–1261.
29 Wicha MS, Liu S, Dontu G. Cancer stem cells: an old idea–a paradigm shift. *Cancer Res* 2006; **66:** 1883–1890; discussion 1895–1896.
30 Clarke MF, Dick JE, Dirks PB, Eaves CJ, Jamieson CH, Jones DL *et al.* Cancer stem cells–perspectives on current status and future directions: AACR Workshop on cancer stem cells. *Cancer Res* 2006; **66:** 9339–9344.
31 Tzivion G, Avruch J. 14-3-3 proteins: active cofactors in cellular regulation by serine/threonine phosphorylation. *J Biol Chem* 2002; **277:** 3061–3064.
32 Matta A, Bahadur S, Duggal R, Gupta SD, Ralhan R. Over-expression of 14-3-3zeta is an early event in oral cancer. *BMC Cancer* 2007; **7:** 169.
33 Lehmann U, Langer F, Feist H, Glockner S, Hasemeier B, Kreipe H. Quantitative assessment of promoter hypermethylation during breast cancer development. *Am J Pathol* 2002; **160:** 605–612.
34 Aitken A. 14-3-3 proteins: a historic overview. *Semin Cancer Biol* 2006; **16:** 162–172.
35 Gardino AK, Smerdon SJ, Yaffe MB. Structural determinants of 14-3-3 binding specificities and regulation of subcellular localization of 14-3-3-ligand complexes: a comparison of the X-ray crystal structures of all human 14-3-3 isoforms. *Semin Cancer Biol* 2006; **16:** 173–182.
36 Morrison R, Schleicher SM, Sun Y, Niermann KJ, Kim S, Spratt DE *et al.* Targeting the mechanisms of resistance to chemotherapy and radiotherapy with the cancer stem cell hypothesis. *J Oncol* 2011; **2011:** 941876.
37 Li Z, Zhao J, Du Y, Park HR, Sun SY, Bernal-Mizrachi L *et al.* Down-regulation of 14-3-3zeta suppresses anchorage-independent growth of lung cancer cells through anoikis activation. *Proc Natl Acad Sci USA* 2008; **105:** 162–167.
38 Ge F, Li WL, Bi LJ, Tao SC, Zhang ZP, Zhang XE. Identification of novel 14-3-3zeta interacting proteins by quantitative immunoprecipitation combined with knockdown (QUICK). *J Proteome Res* 2010; **9:** 5848–5858.
39 Masters SC, Fu H. 14-3-3 proteins mediate an essential anti-apoptotic signal. *J Biol Chem* 2001; **276:** 45193–45200.
40 Qi W, Martinez JD. Reduction of 14-3-3 proteins correlates with increased sensitivity to killing of human lung cancer cells by ionizing radiation. *Radiat Res* 2003; **160:** 217–223.
41 Porter GW, Khuri FR, Fu H. Dynamic 14-3-3/client protein interactions integrate survival and apoptotic pathways. *Semin Cancer Biol* 2006; **16:** 193–202.



Supplementary Information accompanies the paper on Experimental & Molecular Medicine website (http://www.nature.com/emm)